

# Electronic and geometric structures of metal-silicide clusters

M. Sanekata, T. Koya, S. Nagao, Y. Negishi, A. Nakajima, and K. Kaya\*

Department of Chemistry, Faculty of Science and Technology, Keio University,

3-14-1 Hiyoshi, Kohoku-ku, Yokohama 223-8522, Japan

Fax: 81-45-563-5967, e-mail: nakajima@iw.chem.keio.ac.jp

\*Institute for Molecular Science

Fax: 81-564-55-4386, e-mail: kaya@ims.ac.jp

Negative/positive ions of W-silicide cluster are produced by a laser vaporization source for two rods of W and Si. The W-silicide clusters with a metal atom,  $WSi_n$ , are only observed for the size-range of  $n \geq 4$  in the mass spectrum and but are exclusively observed for  $n \geq 6$ . Especially,  $WSi_{15}^{\pm}$  as well as  $WSi_{16}^+$  are remarkably stable comparing with  $WSi_n^{\pm}$  of the neighboring sizes. Photoelectron spectra for their negative ions and the adsorption reactivities toward  $H_2O$  suggest that the stability of  $WSi_n^{\pm}$  for  $n \geq 10$  is due to the geometric structure containing a metal atom.

Key words: metal-silicide cluster, electronic structure, geometric structure, photoelectron, reactivity

## 1. INTRODUCTION

Metal silicides ( $MSi$ ,  $MSi_2$ , and  $M_2Si$  etc.) are extensively used as a Schottky-barrier material at the metal-semiconductor connection in semiconductor devices[1, 2]. Meanwhile, semiconductor clusters and their quantum dots have been known to show size-dependent band gaps due to cluster size/quantum size effect[3]. Metal-silicide clusters are also expected to be as a *cluster material* which show the band gap and the electronic properties with these size dependences.

In this article, we investigate the photoelectron spectra and the adsorption reactivities of W-silicide clusters ( $WSi_n$ ) using the photoelectron spectroscopy for negative ions and chemical probe method for positive ions. The size evolution toward the photoelectron spectra of  $WSi_n^-$  and the adsorption reactivity of  $WSi_n^+$  suggests the existence of the bimodal geometric structures. We will discuss on the stability, connecting with the geometric properties.

## 2. EXPERIMENTAL

The experimental setup was described in detail previously[4, 5]. Briefly, the metal-silicide cluster negative/positive ions are produced by a laser vaporization source. The second harmonics of two Nd:YAG lasers (532 nm) were focused on to a W and a Si rods individually. As for photoelectron spectroscopy for negative ions, the formed negative ions were introduced via a skim-

mer into a time-of-flight (TOF) mass spectrometer. In the photodetachment region, the mass-selected negative ions were photo-detached by the fourth harmonics of a pulsed Nd:YAG laser (266 nm; 4.66 eV). The photoelectron spectra were recorded by measuring the kinetic energy of electrons photo-detached from the negative ion, using a magnetic-bottle type photoelectron spectrometer. While, the adsorption reactivity of  $WSi_n^+$  with  $H_2O$  was examined employing the flow-tube reactor (FTR) combined with the double-rod laser vaporization source[5, 6]. The reactant  $H_2O$  seeded in helium gas at room temperature was injected into FTR, at which a pulsed valve was synchronized with the passing bunch of metal-silicide clusters. In order to estimate the reactivity, the mass spectra were recorded in the presence and absence of reactant.

## 3. RESULTS AND DISCUSSION

### 3.1 Mass Spectroscopy of $WSi_n^-$

Fig.1 shows TOF mass spectra of negative-ion species produced from a double-rod laser vaporization source toward the W and the Si rod. As shown in Fig.1, two major species were found in the mass spectrum. The species are as follows: silicon clusters ( $Si_n^-$ ) in smaller mass range and W-silicide clusters ( $W_mSi_n^-$ ) in larger one. The  $Si_n^-$  clusters have already been known to show the characteristic size distribution resulting from thermal fragmentation[7]. The present  $Si_n^-$  dis-

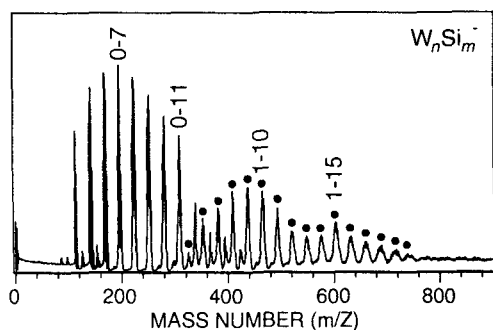


Figure 1: Typical TOF mass spectra of W-silicide cluster negative ions obtained from a double-rod laser vaporization source. The filled circles (●) represent the mass peak for major W-silicide clusters.

tribution observed in this mass spectrum is expected to reproduce the previously reported result. Meanwhile, for W-silicide clusters,  $WSi_n^-$  containing a W atom was only observed in the size range of  $n \geq 4$  and existed dominantly in the size range around  $n \sim 10$ , but no W-silicide cluster containing multiple W atoms was observed throughout the present work. Moreover we unexpectedly found that  $WSi_{15}^-$  was a prominent species comparing with ones of the neighboring sizes. Similar trend has been observed for the positive ions:  $WSi_{15}^+$  and  $WSi_{16}^+$  are stable as quite magic numbers[9, 10]. Comparing  $WSi_n^-$  with  $Si_n^-$ ,  $WSi_n^-$  clusters are expected to be stable with more Si atoms rather than pure  $Si_n^-$ . In order to reveal whether this trend is due to the electric properties or due to the geometric ones, we will discuss the photoelectron spectroscopy of  $WSi_n^-$  in next section.

### 3.2 Photoelectron Spectroscopy of $WSi_n^-$

Fig.2 shows the photoelectron spectra of metal-silicide cluster negative ions  $WSi_n^-$  ( $n = 4-17$ ), using a 266-nm-photodetachment laser. The electron affinities estimated from the appearance thresholds of photoelectron ejection are as shown in Fig.2. The photoelectron spectra of  $Si_n^-$  clusters at 266 nm have been reported in the same size range[11, 12]. The silicon cluster negative ions were categorized into two characters in the neutral electronic structures; closed-shell clusters ( $n = 4, 6, 7, 10$ , and 11) with an isolated small bump in their photoelectron spectra, which enable us to estimate the HOMO-LUMO gap, and open-shell clusters ( $n = 3, 5, 8$ , and 12)

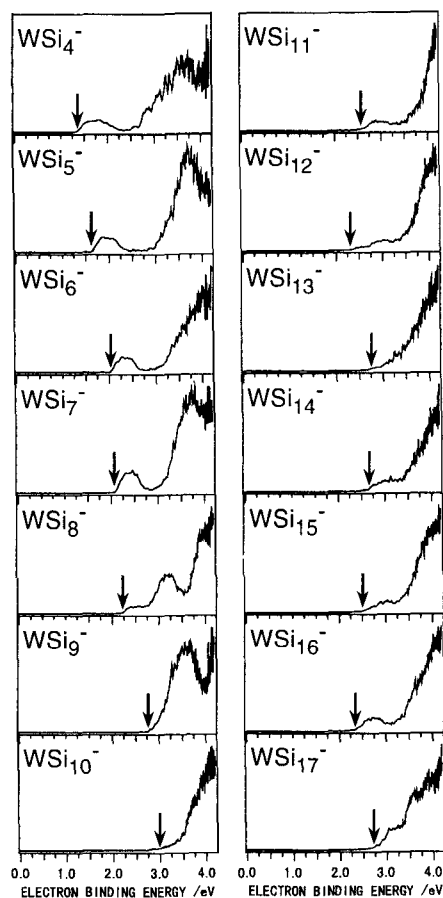


Figure 2: Photoelectron spectra of  $WSi_n^-$  ( $n = 4-17$ ) obtained at 266 nm (4.66 eV). Arrows at the spectral threshold mark the electron affinities.

without the bump.

For  $WSi_n^-$ , the distinct bump is clearly found in the photoelectron spectra for the sizes of  $n = 4-8$ . Then the HOMO-LUMO gaps are expected once to converge into a single peak at  $n = 10$ . For  $n \leq 9$ , the spectral profiles of  $WSi_n^-$  and of  $Si_n^-$  are more alike except for small open-shell clusters of  $n = 3, 5$ , and suggestively 8. In the photoelectron spectra of these open-shell clusters, a new small bump appears. This behavior could be explained by one-electron transfer into a LUMO level of bare silicon cluster from metal atom. On the contrary, the small bump abruptly disappears from the photoelectron spectrum of  $WSi_{10}^-$  although the bump has been observed in the spectra of  $Si_n^-$ . The small-bump vanishing at  $n = 10$  suggests that strong chemical bondings are formed among a W atom and Si atoms, and that  $WSi_{10}^-$  prefers to have some geometric structure with more rich interaction on W-Si.

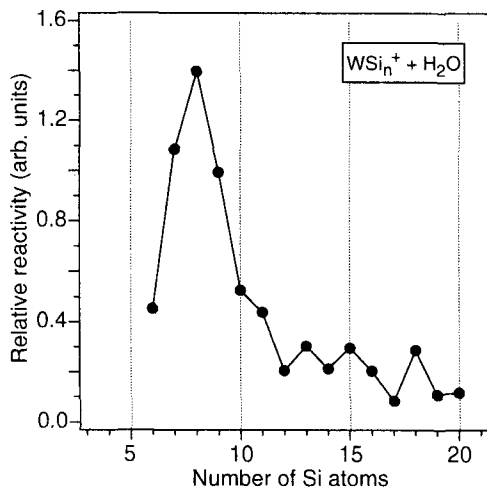


Figure 3: Relative adsorption reactivities of  $\text{WSi}_n^+$  with  $\text{H}_2\text{O}$ .

Over  $n = 11 - 15$ , the bump at threshold is inconspicuous, and the spectral profiles are quite similar to that of  $n = 10$ . These points suggest that  $\text{WSi}_{10}^-$  for  $n \geq 10$  have in common the similar core to  $\text{WSi}_{10}^-$ . In order to conjecture those geometric structures, we examine the adsorption reactivation of W-silicide clusters.

### 3.3 Adsorption reaction of $\text{WSi}_n^+$ with $\text{H}_2\text{O}$

The chemical probe method using FTR has the advantage of roughly estimating the geometric structure and the location where a reactive center is located in/on the cluster[6, 8]. The mass spectra were recorded in the presence/absence of reactant  $\text{H}_2\text{O}$  ( $\sim 0.6\%$ ) seeded in helium gas. As the mass peak of prepared clusters is  $I_0$  and one of remaining clusters  $I$ , the reactivity  $R$  is described by  $R = -\ln(I/I_0)$ .

Fig.4 shows the reactivity of  $\text{WSi}_n^+$  clusters with  $\text{H}_2\text{O}$  obtained from the chemical probe experiment. This size-dependent reactivity is roughly divided into two regions; (1) high reactivities for  $7 \leq n \leq 9$  and (2) relatively smaller ones for  $n \geq 10$ . These trends are quite similar between  $\text{WSi}_n^-$  and  $\text{WSi}_n^+$  independent of their charges[14]. The reactivities of  $\text{Si}_n^+$  with  $\text{H}_2\text{O}$  and  $\text{D}_2\text{O}$  provide us with a hint to understand the interaction of  $\text{WSi}_n^+$  clusters with  $\text{H}_2\text{O}$ . According to previously reported results of  $\text{Si}_n^+$ , the reactivity for  $n \leq 6$  decreases with  $n$  and one for  $n = 5$  and 6 is negligibly small[13]. While, the reactivity for  $n = 10 - 30$  strongly shows the size-dependence, and especially  $\text{Si}_{11}^+$ ,

$\text{Si}_{13}^+$ ,  $\text{Si}_{14}^+$ ,  $\text{Si}_{19}^+$ , and  $\text{Si}_{23}^+$  are unreactive[8]. Therefore, as shown in Fig.4, the behavior for reactivity of  $\text{WSi}_n^+$  is quite different from that of  $\text{Si}_n^+$ . Consequently, this is suggested that the reactivity of  $\text{WSi}_n^\pm$  is drastically affected by the W- $\text{H}_2\text{O}$  interaction. Indeed, we observed the striking reaction of  $\text{W}^+$  with  $\text{H}_2\text{O}$  in the mass spectrum;  $\text{W}^+ + x(\text{H}_2\text{O}) \rightarrow \text{WO}_n^+$  ( $n = 1 - 3$ ). Assuming that W atom behaves as a reaction center, the behaviors of the size-dependent reactivities for (1) and (2) as mentioned above are easily understandable. However, it is impossible to explain the abrupt depression at  $n = 10$ . For negative ions as shown in Fig.4, we observed quite similar behavior for the size-dependent reactivity, although the signal intensities were far lower in the chemical-probe experiment for negative ions than for positive ions. It is conjectured that the depression at  $n \geq 10$  is due to geometric structure rather than due to the electronic structure, and that the geometric structure at  $n \geq 10$  changes suddenly into the structure that the reaction-centered metal is besieged by silicon atoms. As mentioned previously, the photoelectron spectra of  $n = 10$  feasibly indicate the structural change. For  $n = 10$ , the interstitial structure, which prefers the direct W-Si interaction, should be supported in this work as S. M. Beck said[9, 10]. In the same way as  $n = 10$ , another  $\text{WSi}_n^\pm$  clusters for  $n \geq 10$  consist of such metal-centered structure. The drastical change at  $n = 10$ , which the location of metal atom transfers from the surface to the inside of  $\text{Si}_n$  cluster, is expected to involve with as a microscopic phase transition in silicide crystals. For  $\text{WSi}_{15}$  behaving as a magic number, the cluster is stabilized from the geometric property rather than electronic ones because there is no serious difference among the photoelectron spectra of  $n = 14 - 15$ . At present, we also have no results on the structure of  $\text{WSi}_{15}^\pm$  supported by theoretical calculation. However  $\text{WSi}_{15}^\pm$  structure is expected to be close to the substitutional one consisting of  $\text{WSi}_{16}$  unit extracted from diamond structure of bulk Si crystal.

## 4. CONCLUSIONS

In this article, we have investigated the electronic and geometric structures of the W-silicide clusters,  $\text{WSi}_n^\pm$ , using the photoelectron spectroscopy and the chemical-probe method. Both of the photoelectron spectra for negative ions and the chemical reactivities with  $\text{H}_2\text{O}$  indicate that a W atom is located on the surface of Si

cluster for  $n \leq 9$  and in the network of Si cluster for  $n \geq 10$ . In the latter clusters, the  $\text{WSi}_{15}^-$  is particularly stable as a magic cluster. This stability for  $n = 15$  as well as  $n \geq 10$  is attributed to arising from the geometric structure rather than the electronic one. These behaviors may be concerned in the microscopic feature toward the infiltration of metal impurity into silicon crystal.

#### ACKNOWLEDGEMENTS

This work was supported by a program entitled "Research for the Future" of the Japan Society for the Promotion of Science (No. 98P01203) and by a Grant-in-Aid for Scientific Research (No. 12740326) from the Ministry of Education, Science and Culture of Japan.

#### REFERENCES

- [1] S. M. Sze, *Physics of Semiconductor Devices*, Wiley, New York, 1981.
- [2] W. Mönch, *Surf. Sci.* 299/300 (1994) 928.
- [3] S. V. Gaponenko, *Optical Properties of Semiconductor Nanocrystals*, Cambridge Univ. Press, 1998.
- [4] A. Nakajima, T. Taguwa, K. Hoshino, T. Sugioka, T. Naganuma, F. Ono, K. Watanabe, K. Nakao, Y. Konishi, R. Kishi, K. Kaya, *Chem. Phys. Lett.* 214 (1993) 22.
- [5] S. Nagao, T. Kurikawa, K. Miyajima, A. Nakajima, K. Kaya, *J. Phys. Chem. A* 102 (1998) 4495.
- [6] M. E. Guesic, M. D. Morse, S. C. O'Brien, R. E. Smalley, *Rev. Sci. Instrum.* 56 (1985) 2123.
- [7] L. A. Bloomfield, M. E. Geusic, R. R. Freeman, W. L. Brown, *Chem. Phys. Lett.* 121 (1985) 33.
- [8] U. Ray, M. F. Jarrold, *J. Chem. Phys.* 94 (1991) 2631.
- [9] S. M. Beck, *J. Chem. Phys.* 90 (1989) 6306.
- [10] S. M. Beck, *Advances in Metal and Semiconductor Clusters*, 1 (1993) 241.
- [11] O. Cheshnovsky, S. H. Yang, C. L. Pettiette, M. J. Craycraft, Y. Liu, R. E. Smalley, *Chem. Phys. Lett.* 138 (1987) 119.
- [12] H. Kawamata, Y. Negishi, R. Kishi, S. Iwata, A. Nakajima, K. Kaya, *J. Chem. Phys.* 105 (1996) 5369.
- [13] W. R. Creasy, A. O'Keefe, J. R. McDonald, *J. Phys. Chem.* 91 (1987) 2848.
- [14] M. Sanekata, S. Nagao, Y. Negishi, T. Koya, A. Nakajima, K. Kaya, *to be submitted*

(Received December 17, 1999; Accepted August 31, 2000)